Volume 3 | Number 10 | October 2016

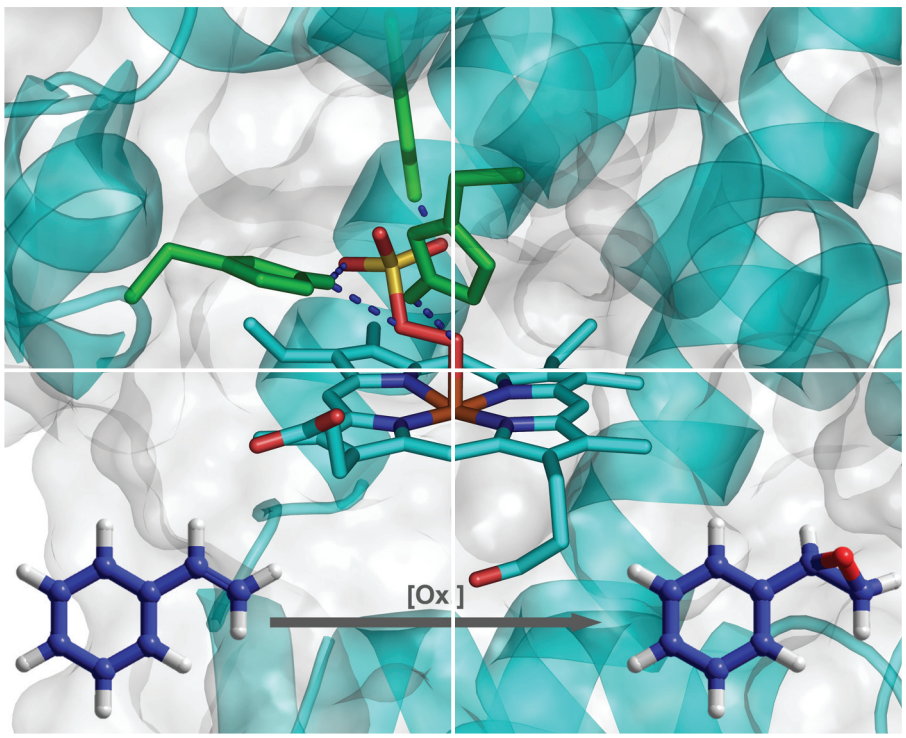

INORGANIC CHEMISTRY

FRONTIERS

Chinese Chemical Society

ROYAL SOCIETY OF CHEMISTRY

http://rsc.li/frontiers-inorganic

INORGANIC CHEMISTRY
FRONTIERS

RESEARCH ARTICLE

View Article Online
View Journal | View Issue

Cite this: *Inorg. Chem. Front.*, 2016, **3**, 1236

Manganese protoporphyrin IX reconstituted myoglobin capable of epoxidation of the C=C bond with Oxone®†

Yuan-Bo Cai,[a] Si-Yu Yao,[a] Mo Hu,[b] Xiaoyun Liu*[b] and Jun-Long Zhang*[a]

Received 9th May 2016,
Accepted 11th August 2016

DOI: 10.1039/c6qi00120c

rsc.li/frontiers-inorganic

Replacement of the native heme cofactor by manganese protoporphyrin IX (MnPPIX) to reconstitute manganese myoglobin (Mn^{III}Mb) is an important approach to investigate the reactivity of the Mn center inside protein scaffolds. However, unlike the Mn porphyrin synthetic model compounds, MnPPIX reconstituted myoglobins (Mn^{III}Mb) have no reactivity in the epoxidation of styrene using H_2O_2, which was attributed to the low reactivity of the Mn^{IV}=O intermediate after homocleavage of the O–O bond in manganese peroxide. To address this issue, we herein chose Oxone® ($2KHSO_5 \cdot KHSO_4 \cdot K_2SO_4$), a well-known oxidant undergoing O–O bond heterocleavage. After screening 7 mutants and wild-type Mn^{III}Mb, we found that the L29H/F43H mutant could generate a new species ($[Mn^{IV}=O]^{+\bullet}$), tentatively assigned by using UV-vis and EPR spectra, through heterocleavage of the O–O bond. Computational docking showed hydrogen bonds between three distal histidines (H64, L29H and F43H) and anions, which increase the binding affinity to persulfate. With Oxone® as the oxidant, Mn^{III}Mb (L29H/F43H) showed the highest reactivity toward the epoxidation of styrene, different from that with the H_2O_2 oxidant. This work demonstrates the first example of MnPPIX reconstituted Mb which could catalyze styrene epoxidation and provides new insights to further explore the reactivity of the Mn center in protein scaffolds.

Introduction

Manganese (Mn) is an important redox cofactor widely found in many metalloproteins or metalloenzymes such as the oxygen evolution cluster (OEC) in photosynthetic system II,[1,2] superoxide dismutases (SOD),[3] and catalases.[4] In sharp contrast to iron (Fe), few Mn protoporphyrin complexes have been used as cofactors in naturally redox metalloproteins, although their synthetic analogues such as Mn(III) and Fe(II) porphyrins displayed comparable catalytic reactivity in oxygen atom transfer reactions.[5–10] To decipher their different reactivities inside protein scaffolds, replacing the heme cofactor with Mn analogues in heme containing metalloproteins thus became an emerging approach to deepen the understanding of the structural relationship of redox reactivity, expand the repertoire of metalloenzyme catalyzed reactions and even enrich our knowledge of nature's choice for metal cofactors.

Toward this goal, Mn protoporphyrin IX (MnPPIX) reconstituted heme containing metalloproteins, including horseradish peroxidase,[11–13] cytochrome *c* peroxidase,[14,15] microperoxidase-8 [16–19] and myoglobin,[20–27] have been extensively studied. Especially inside myoglobin, the comparative studies of the structure,[20] electrochemical properties,[21,28] Raman spectra,[23] electron paramagnetic resonance (EPR),[24,29] and redox reactivity[22,25–27,30] of MnPPIX with heme provided valuable insights to understand the relationship between the intrinsic electronic structures and the redox reactivities. Prominently, Watanabe,[31] Hayashi[32] and Lu[33–35] reported that replacement of heme with Mn porphycene or salen complexes afforded new Mn myoglobins capable of catalyzing oxygen atom transfer reactions even in good enantioselectivity, which revealed the potential applications of Mn reconstituted myoglobins in organic catalysis. Despite the tremendous progress made in the past few years, most MnPPIX reconstituted metalloproteins exhibited peroxidase like reactivity,[36–38] other than the reactivity in oxygen atom transfer reactions such as epoxidation of the C=C bond, sulfoxidation and hydroxylation of C–H bonds.[39] To address this issue, we herein reported the first example of MnPPIX reconstituted myoglobin (L29H/F43H), capable of catalyzing epoxidation of the C=C bond (styrene) with Oxone®.

[a]*Beijing National Laboratory for Molecular Sciences, State Key Laboratory of Rare Earth Materials Chemistry and Applications, College of Chemistry and Molecular Engineering, Peking University, Beijing 100871, P. R. China. E-mail: zhangjunlong@pku.edu.cn; Fax: (+86) 10-62767034*
[b]*Institute of Analytical Chemistry and Synthetic and Functional Biomolecules Center, College of Chemistry and Molecular Engineering, Peking University, Beijing 100871, P. R. China. E-mail: xiaoyun.liu@pku.edu.cn; Fax: (+86) 10-62759813*
†Electronic supplementary information (ESI) available. See DOI: 10.1039/c6qi00120c

Different reactivities between the active intermediates [Fe^{IV}=O] (less active, Comp. II) and [Fe^{IV}=O]$^{+\bullet}$ (more active, Comp. I) have been found in myoglobins, which are generated through homo- and heterocleavage of the O–O bond in iron(III) peroxide, respectively. Especially for the latter, the [Fe^{IV}=O]$^{+\bullet}$ species was believed to be the real active intermediate in many catalytic oxygen atom transfer reactions.[40–43] However, MnPPIX had been reported to generate a low active [Mn^{IV}=O] intermediate inside the myoglobin scaffold, which could not oxidize styrene but ABTS, with typical reactivity like peroxidases.[38] Thus, we hypothesized that the intermediate [Mn-OOH] inside myoglobin tends to undergo homocleavage of the O–O bond. Thus, looking for an appropriate oxidant to produce active [Mn^{V}=O] or [Mn^{IV}=O]$^{+\bullet}$ intermediate(s) through heterocleavage of the O–O bond is of importance. To test this hypothesis, we herein chose Oxone® as the oxidant, because it is well-known to react with the Mn center through heterocleavage of the O–O bond.[5,6,44–47] Moreover, Oxone® has low pK_a and exists in the anionic form under physiological conditions, which is favorable to bind the Mn cation center. To optimize the secondary coordination sphere, we designed several mutants (L29H, F43H, H64F, L29H/H64F, F43H/H64F, L29H/F43H and L29H/F43H/H64F). As shown in UV-vis spectroscopic titration, only the L29H/F43H mutant (His3 Mn^{III}Mb) showed the formation of the Mn-oxo type intermediate with a broad absorption centered at *ca.* 623 nm, which might be arising from the Mn^{IV}-oxo cation radical. EPR studies for the reaction between His3 Mn^{III}Mb and Oxone® showed both the radical signal at g = 2.00 and the Mn^{IV} signal at g = 4.30. These results clearly suggested the generation of different Mn-oxo intermediates in Mb (L29H/F43H) between Oxone® and H_2O_2. Computational docking of the HSO_5^- ion to the cavity of His3 Mb (PDB code: 4FWZ)[48] demonstrates that three distal histidines bind the persulfate anion through hydrogen bonds, which might increase the binding affinity as well as promote the O–O bond cleavage. Interestingly, the reactivity assay for epoxidation of styrene demonstrated that Mn^{III}Mb (L29H/F43H) with Oxone® has the highest reactivity (48 ± 2 × 10^{-3} turnover per min) and the main product is styrene epoxide. Therefore, this work provides an access to understand the oxidation mechanism for MnPPIX inside myoglobin scaffolds and explore the potential application in oxygen atom transfer reactions.

Results and discussion

Reactions of Mn^{III}Mbs and Oxone®

To optimize the secondary coordination sphere for the reaction between the Mn center and Oxone®, we herein focused on the different combinations of distal histidines (Fig. 1 and Table 1) such as Leu-29, Phe-43, and His-64, according to our and other's previous reports.[33,38,41,49] Construction of these Mn Mb mutants was carried out following our previous procedures, and UV-vis absorption and mass spectra were identical.[38]

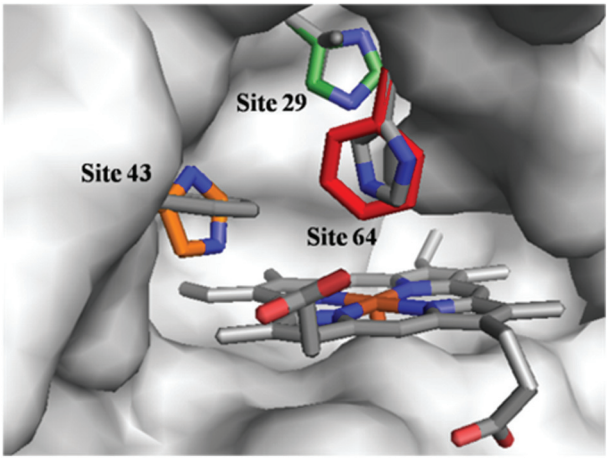

Fig. 1 Structures of the heme pocket of sperm whale myoglobin (gray). And the residues mutated in our studies are also shown: His-29 (green), His-43 (orange), and Phe-64 (red). All N atoms are marked in blue. The PDB code for wild-type Mb is 1JP6. Structures of mutants were reproduced by PyMol.

Table 1 Residues at sites 29, 43, and 64 of wild-type Mb and different mutants

	Residues		
Myoglobin mutants	Site 29	Site 43	Site 64
Wild-type	Leu	Phe	His
F43H	Leu	His	His
L29H	His	Phe	His
H64F	Leu	Phe	Phe
L29H/F43H (His3)	His	His	His
F43H/H64F	Leu	His	Phe
L29H/H64F	His	Phe	Phe
L29H/F43H/H64F	His	His	Phe

The reactions of Mn^{III}Mbs with 100 eq. Oxone® (containing 200 eq. $KHSO_5$) were carried out and monitored by UV-vis absorption spectroscopy in 50 mM potassium phosphate buffer (pH = 7.4) at 20 °C. As shown in Fig. 2a, b and S2–7,† only the L29H/F43H mutant (His3 Mn^{III}Mb) displayed a decrease in the absorption at 376, 471 and 550 nm, and an appearance of a single Soret band at 411 nm. In Fig. 2a, the reaction between His3 Mn^{III}Mb and Oxone® resulted in nearly isosbestic conversion in the initial stage (0–500 s) and the kinetic trace obeyed pseudo first-order kinetics. This clearly indicates that the combination of three distal histidines (L29H, F43H and H64) is more effective to activate the reaction with Oxone® compared to the other mutants and wild-type Mn^{III}Mb. Notably, a broad shoulder centered at 623 nm appeared, indicating the formation of the Mn^{IV} porphyrin π cation radical according to those found in some synthetic porphyrinoid ligands.[50–52] In our previous work using H_2O_2 to oxidize His3 Mn^{III}Mb,[38] no such broad shoulder at *ca.* 623 nm was observed. It is worth noting that Stone and co-workers reported similar spectral changes when they used *m*-CPBA as the two-electron oxidant.[30] To confirm that the new species is

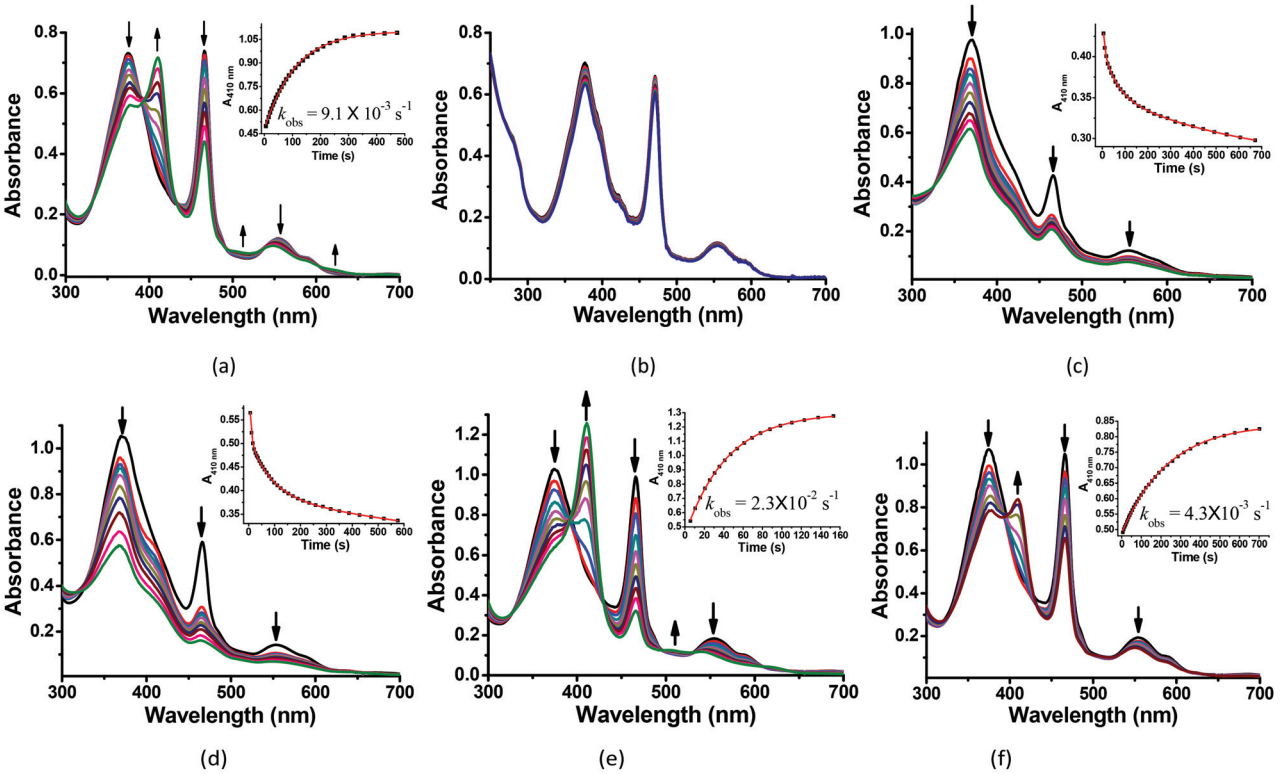

Fig. 2 Kinetic studies of 30 μM (a) His3 Mn^{III}Mb and (b) wild-type Mn^{III}Mb reacted with 200 equiv. $KHSO_5$ in PBS buffer (pH = 7.4). And 30 μM His3 Mn^{III}Mb reacted with 200 equiv. $KHSO_5$ at (c) pH = 5.1, (d) pH = 6.0, (e) pH = 7.0, and (f) pH = 8.0. Inset: Time course plots of absorbance at *ca*. 410 nm, attributing to the formation of the Mn=O intermediate.

Oxone® dependent, we reduced the amount of Oxone® to 20 equiv. (Fig. S1†) and found that a smaller amount of new species formed with a slower reaction rate (k_{obs}) of 2.8 × 10^{-3} s^{-1} (*vs.* 9.1 × 10^{-3} s^{-1} with 200 equiv. $KHSO_5$, reaction time: 0–500 s). This suggested the generation of an intermediate like the Mn^{IV}-oxo cation radical or the protein radical using the Oxone® oxidant.

We then investigated the pH effect (pH 5.1, 6.0, 7.0 and 8.0) on the reaction between Oxone® and His_3 Mn^{III}Mb, and UV-vis spectra are shown in Fig. 2c–f. At low pH values (5.1 and 6.0), UV-vis spectra showed fast disappearance of Soret and Q bands, with a slight increase of absorption at 411 nm. This might be due to MnPPIX bleaching or slipping out of the protein scaffold. We ascribed the low stability to the protonation of distal histidines (pK_a *ca*. 6.0), which likely alters the H-bonding interactions in the distal pocket or even the configuration of the protein scaffold. In contrast to that, higher pH values (7.0, 7.4 and 8.0) showed the typical UV-vis spectra of the Mn^{IV}-oxo cation radical with a negligible absorption decrease, indicating that high valent [Mn^{V}=O] or [Mn^{IV}=O]$^{+\bullet}$ species may be stabilized under basic conditions.[53] When pH ≥ 7, the reaction rates (first order kinetic rate) also decreased along with the increase of pH. Under the incubation with 6 mM Oxone, His_3 Mn^{III}Mb displays much faster (2.3 × 10^{-2} s^{-1} at 20.0 °C) at pH 7 than those at higher or lower pH.

Docking HSO_5^- to His3 Mb

Oxone® is a mixture of $KHSO_5{\cdot}0.5KHSO_4{\cdot}0.5K_2SO_4$ and the active species is potassium hydrogen persulfate ($KHSO_5$). To understand the role of distal histidines (L29H, F43H and H64) in activating Oxone®, we carried out a computational study for docking HSO_5^- to the His3 cavity above the MnPPIX in myoglobin. The model myoglobin we chose is His3 Mb (PDB code: 4FWZ) reported by Lu and co-workers.[48] We replaced the heme cofactor by the MnPPIX complex and removed water molecules in the crystal data. For the low pK_a of hydrogen persulfate, the proton was supposed to transfer to His-64. As shown in Fig. 3, hydrogen bonding interactions are observed between terminal oxygens and His-29 and His-43, with the distance of 1.60 and 1.86 Å, respectively. The proximal oxygen in hydrogen persulfate could form hydrogen bonds with His-43 and protonated His-64, with the distance of 2.13 and 2.51 Å, respectively. The distance between the H atom of His64 and the O atom of hydrogen persulfate proximal to the Mn center is 3.15 Å, which is a little longer than the normal hydrogen bond. And the N–H in His64 was directly towards the uncoordinated O atom. Thus, we considered that the H-bond was only between His-64 and the distal O atom of peroxide. Thus, this docking experiment tentatively interprets that three distal histidines facilitate HSO_5^- binding to the cavity above MnPPIX through

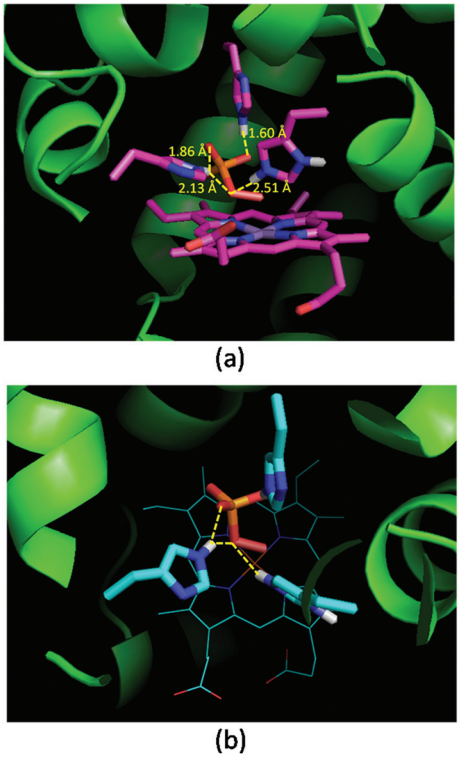

Fig. 3 Docking results of His3 Mn^{III}Mb and HSO_5^-. (a) Side view, (b) top view. Hydrogen bonds and distances of three histidines and oxygens in HSO_5^- are labelled in (a).

cooperative hydrogen bonding, which might assist the consequent O–O bond heterocleavage.

EPR studies for the reaction of His3 Mn^{III}Mb and Oxone®

To characterize intermediates in the reaction between Oxone® and His3 Mn^{III}Mb, we carried out EPR experiments to monitor the reaction process according to the work by Yonetani[54] and Hori.[55] In this study, we used H_2O_2 as a control. 10 eq. Oxone® (containing 20 eq. $KHSO_5$) was added to the solution of His3 Mn^{III}Mb (1.0 mM) in PBS buffer (pH 7.4). The reaction lasted for 3 min at 4 °C, and then quickly frozen with liquid nitrogen. As shown in Fig. 4a, His3 Mn^{III}Mb reacted with $KHSO_5$ and showed a Mn^{IV} signal at g = 4.30 and a characteristic sharp signal at g = 2.00 which was assigned to the protein radical or porphyrin π cation radical. Similarly, 20 eq. of H_2O_2 was used with the same procedure, and only the Mn^{IV} signal at g = 4.30 was observed (Fig. 4b), consistent with the previously reported homocleavage of the O–O bond of Mn peroxide.[27,38,56] As shown in Fig. 4c, in the absence of oxidant, no signal was observed at both g = 2.00 and 4.30.

In addition, the reaction between Oxone® and apo-myoglobin did not afford such a radical signal at g = 2.00 (Fig. 4d). Thus, the signal at g = 2.00 could be assigned to either protein radicals such as Tyr and Trp through one-electron oxidation[11] or porphyrin π cation radicals. Nevertheless, these EPR results clearly indicate the different Mn-oxo species generated by Oxone® from that by H_2O_2.

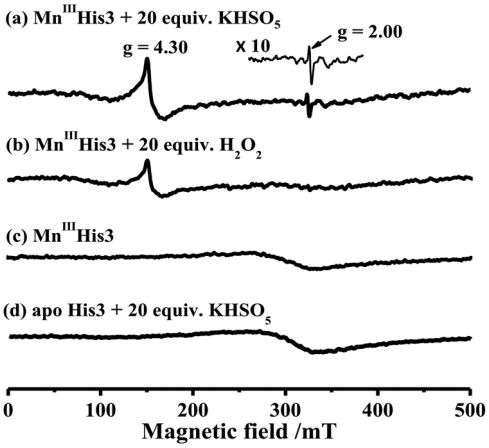

Fig. 4 X-band EPR spectra of (a) 1.0 mM His3 Mn^{III}Mb in 50 mM PBS buffer (pH 7.4), and (b) in the presence of 20 equiv. H_2O_2 or (c) 20 equiv. $KHSO_5$, and (d) apo-His3 Mb in the presence of 20 equiv. $KHSO_5$. The EPR spectra are recorded at –170 °C.

Post-oxidation of protein scaffold by Oxone®

To further identify the oxidation of the protein scaffold by Oxone®, we performed ESI-MS spectrometry to characterize the molecular weight immediately after the reaction of Oxone® and His3 Mn^{III}Mb for 3 min. The fitting results show two peaks at 17 376 and 17 390 Da (Fig. 5), which correspond to the addition of 2 and 3 oxygen atoms to the His3 Mb (M = 17 345 Da), respectively. This indicates that the protein scaffold was oxidized with the addition of 2 or 3 oxygen atoms using 20 eq. Oxone®. The reaction of Oxone® with apo-myoglobin was used as control (Fig. S8†) and no oxidized protein was found in ESI-MS, indicating that the oxidation of the protein scaffold by $KHSO_5$ only occurs in the presence of the MnPPIX cofactor.

We then used LC-MS/MS to identify the oxidized amino acid residues. His3 Mn^{III}Mb was reacted with Oxone® for 3 min. H_2O_2 was used as a control oxidant, and apoprotein was taken as a blank to exclude the possible oxidation occurring in LC-MS/MS treatments. The normalized peak areas were calculated by the ratio of oxidized/unoxidized peptides, which

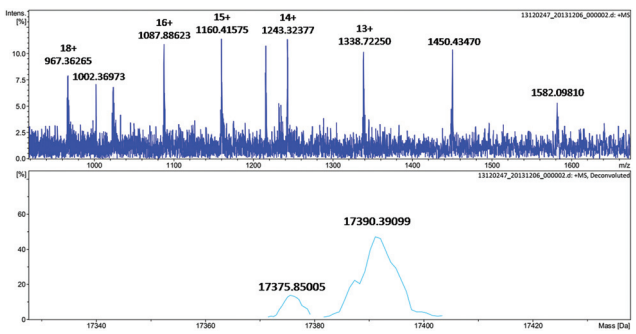

Fig. 5 ESI-MS of His3 Mn^{III}Mb after reacting with 20 equiv. $KHSO_5$ for 3 min.

Table 2 Comparison of oxidized peptides found in trypsin autolysis products

Peptides	Observed *m/z*	Theoretical *m/z*	Delta	Normalized Area: Apo-His3 Mb + Oxone®	His3 Mn^{III}Mb	His3 Mn^{III}Mb + Oxone®	His3 Mn^{III}Mb + H_2O_2
HPGDFGADAQGAM(OX)NK	766.52	766.81	−0.29	3.2×10^6	4.6×10^6	1.1×10^7	3.9×10^6
HLKTEAEM(OX)K	368.38	368.43	−0.05	3.8×10^4	3.6×10^4	1.2×10^6	4.7×10^4
YKELGY(OX)QG	487.37	487.53	−0.16	1.5×10^6	1.5×10^6	4.3×10^6	1.6×10^6

Table 3 Reaction rate of different proteins catalyzed by styrene epoxidation[a]

Entry	Catalyst	Rate[b]
1	No catalyst	N.D.[c]
2	MnPPIX	N.D.[c]
3	Apo-His3 Mb	N.D.[c]
4	His3 Mn^{III}Mb	48 ± 2
5	His3 Fe^{III}Mb	15 ± 2
6	F43H Mn^{III}Mb	11 ± 1
7	Wild-type Mn^{III}Mb	5.4 ± 0.4
8	His3 Mn^{III}Mb (with H_2O_2)[d]	N.D.[c]

[a] Reaction conditions: 0.2 mM proteins, 4 mM styrene and $KHSO_5$ in 50 mM PBS buffer (pH = 7.4) at 4 °C, reacting for 1 h. [b] The unit of rate is 10^{-3} turnover per min. [c] The epoxidation product was not detected. [d] Reaction with H_2O_2 instead of $KHSO_5$ as oxidants.

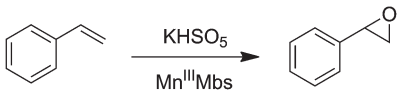

Scheme 1 Styrene epoxidation by $KHSO_5$.

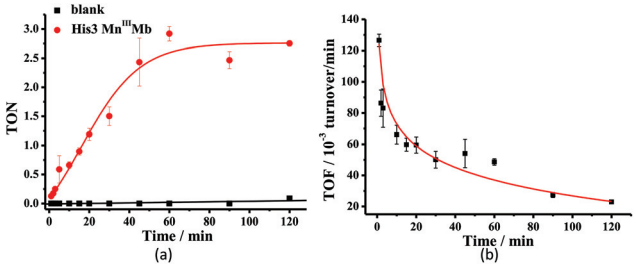

Fig. 6 Time course plots of (a) turnover number (TON) with or without His3 Mn^{III}Mb, and (b) turnover frequency (TOF) of styrene epoxidation catalyzed by His3 Mn^{III}Mb. TON and TOF were calculated based on the amount of styrene. The initial TOF was calculated at 1 min.

was used to estimate the degree of oxidization. As shown in Tables 2 and 3 peptides were found to be oxidized by $KHSO_5$. We found that the fragmentation patterns of the peptide were HPGDFGADAQGAM(Ox)NK, as shown in Fig. S9 and 10.† According to the peptide sequences, oxidation mainly occurred at Met-55, Met-131 and Tyr-151. It's noteworthy that reacting with H_2O_2 or apo-His3 Mb in the presence of $KHSO_5$ does not generate remarkable oxidations. They only show slightly increasing contents on Met-55. This indicates that a quick post-oxidation by a high reactive Mn-oxo intermediate with Oxone® could oxidize the residues inside the protein scaffold, which is in accordance with the EPR experimental results. These three residues were distant from the Mn center and localized near the surface, which was probably because of the radical transfer through some residues from the cavity to the surface.

Epoxidation activity

Mn porphyrins are well known catalysts in oxygen-atom transfer (OAT),[6–10] hydrogen-atom transfer (HAT),[57,58] and electron transfer (ET) reactions,[59,60] and Mn^{V}-oxo or/and $[Mn^{IV}{=}O]^{+\bullet}$ species were proposed as active intermediates. Since the reaction of Oxone® and Mn His3 Mb could generate more active Mn-oxo species, it is very important to investigate the reactivity toward oxygen atom transfer reactions. In this work, we chose styrene as the substrate, and Oxone® as the oxidant to examine the catalytic reactivity of these Mn^{III}Mbs (Scheme 1, Table 3). As shown in Fig. S11,† styrene epoxide is the main product. And the time course experiment of styrene epoxidation catalyzed by His3 Mn^{III}Mb (Fig. 6a) shows that the reaction ends in about 1 h. The initial TOF (turnover frequency) is up to 1.30×10^{-1} under the same conditions. Changing Oxone® to H_2O_2, His3 Mn^{III}Mb showed no reactivity toward epoxidation of styrene (entry 8).

Among the Mn^{III}Mb mutants and wild-type Mn^{III}Mb, His3 Mn^{III}Mb shows the highest reaction rate ($48 \pm 2 \times 10^{-3}$ turnover per min, entry 4,) with Oxone® as the oxidant, which is 8.9 times higher than wild-type Mn^{III}Mb ($5.4 \pm 0.4 \times 10^{-3}$ turnover per min, entry 7), 4.4 times higher than F43H Mn^{III}Mb ($11 \pm 1 \times 10^{-3}$ turnover per min, entry 6), and even 3.2 times higher than His3 Fe^{III}Mb ($15 \pm 2 \times 10^{-3}$ turnover per min, entry 5). Other mutants are not reactive toward epoxidation of styrene under these reaction conditions. The trend observed in the epoxidation of styrene is similar to that in the UV-vis spectra for the reactions between Mn^{III}Mbs and Oxone®, suggesting the correlation between the formation of Mn-oxo intermediate(s).

We also investigated the pH effect on the epoxidation of styrene, since the formation of $Mn^{IV/V}$-oxo was pH dependent. As shown in Fig. S12,† at pH 7.0 and pH 7.4, the reactivity toward the epoxidation of styrene is much higher than those obtained at lower pH (<7) or higher pH (>7.4), which is quite in line with the UV-vis studies for pH effects. In addition, we examined the enantioselectivity of styrene epoxide catalyzed by His3 Mn^{III}Mb and low enantioselectivity (<10%) was detected.

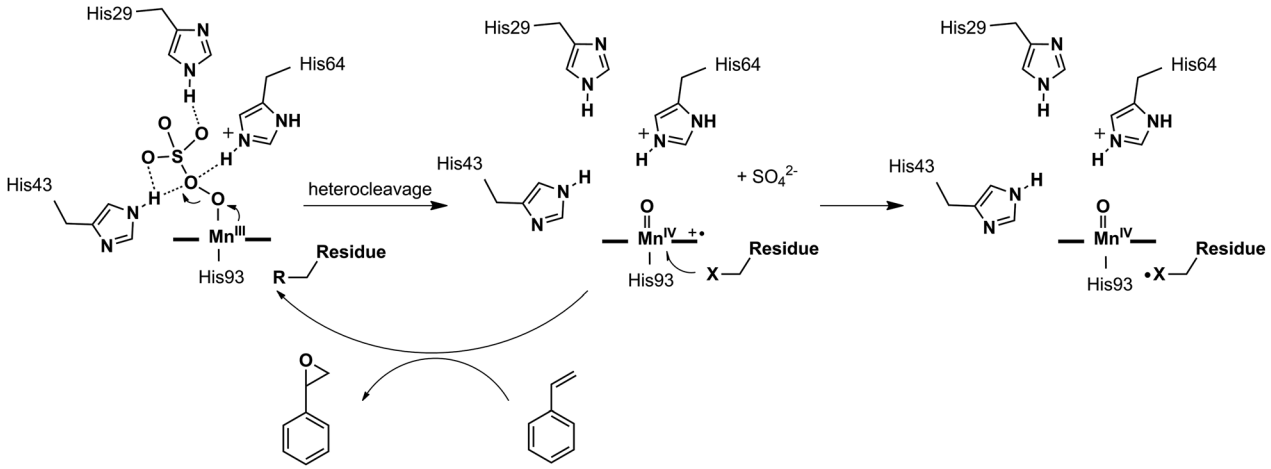

Scheme 2 Proposed mechanism of the formation of the Mn-oxo intermediate, styrene epoxidation, and oxidation of protein amino acid residues.

Finally, we used ethylbenzene as the substrate to test the reactivity of His3 Mn^{III}Mb and Oxone® and no oxidation of the C–H bond was obtained. Nevertheless, the reactivity of His3 Mn^{III}Mb and Oxone® toward styrene epoxidation reveals the potential of this protocol for further application in oxygen atom transfer reactions.

The possible reaction mechanism

In this work, we demonstrated the ability of Mn reconstituted Mb to oxidize the C=C bond using Oxone® as the oxidant. We proposed the possible mechanism of the generation and subsequent reactions of the Mn-oxo intermediate as in Scheme 2. The coordination of HSO_5^- ions to Mn was stabilized by hydrogen bonds with His-29, His-43, and His-64. Then the Mn^V-oxo intermediate was generated by O–O bond heterocleavage. This highly active intermediate could oxidize substrates such as styrene, or oxidized residues like tyrosine to form protein radicals. On the other hand, distal histidine plays a critical role in activating Oxone® as we mentioned above. Previously, Watanabe and co-workers revealed that the location of single distal histidine affects the activation process of H_2O_2 in myoglobin.[41] Recently, we reported the cooperative effect of dual distal histidines at positions 64 and 43 on the activation of H_2O_2 with the Mn center within the myoglobin scaffold, which might be due to the higher pK_a of H_2O_2 binding to Mn than that of the Fe center.[38] For the effects of three distal histidines, Lin and co-workers reported that Cu binding to His3 Mb inhibits the peroxidase activity, which thus suggests their essential role in the activation of the oxidant.[61] In this work, we demonstrated the essential role of three distal histidines in activating Oxone, a two-electron oxidant, *via* heterocleavage of the O–O bond. This is in line with the previous studies and highlights the importance of distal histidines in designing artificial metal oxidases. Thus, the next step to improve this catalytic system would include how to avoid the decomposition of MnPPIX and self-oxidation of protein scaffolds, which are further important to enhance the reactivity and reaction turnover numbers.

Conclusions

Altogether, we described the first example of design of manganese reconstituted myoglobin, which is reactive toward oxygen atom transfer reactions with Oxone® as the oxidant. There are two critical factors to determine this kind of reactivity. One is to find an appropriate oxidant, which undergoes heterocleavage of the O–O bond of Mn peroxide to generate more active $[Mn^{IV}{=}O]^{+\bullet}$ intermediate(s) other than the low reactive Mn^{IV}=O intermediate generated by H_2O_2. The next is the secondary coordination sphere, which is constructed by three distal histidines (L29H, F43H and H64) in this work. Compared to our previous work in which two histidines (H64 and F43H) could bind H_2O_2 and deprotonate proximal hydrogen and generate Mn^{IV}=O,[38] the activation of Oxone® required three distal histidines to form a cooperative hydrogen bond with the terminal oxygen atom. Obviously, more charge separation between the O–O bond is favourable to such bond hetero-cleavage. More importantly, His3 Mn^{III}Mb has the ability to oxidize styrene, which reveals the perspective on engineering metalloproteins by changing metal cofactors and tuning the secondary coordination sphere, and brings new insights into design of more effective metalloproteins with functions not found in nature.

Materials and methods

General

All chemicals including protoporphyrin IX, Oxone® and styrene were purchased from Alfa Aesar and used without further purification. Manganese(III) protoporphyrin IX and different Mbs were prepared according to the previous reports.[38] ESI-MS spectra were recorded with a Bruker Apex IV FTMS spectrometer. LC-MS/MS was performed on a LTQ Velos Pro dual-pressure linear ion trap liquid Chromatography Mass Spectrometer. UV-vis spectra were recorded with an Agilent 8453 UV-Vis spectrometer. Continuous wave X-band EPR

spectra were recorded on a Bruker ER200D-SRC X-band spectrometer with irradiation at 9.042 GHz and 7.99 mW. Gas chromatography was performed on an Agilent 7890A gas chromatograph with an FID detector. The yield was detected by using a 30 m × 0.32 mm^2 HP-5 column, and the enantioselectivity was determined by using a 30 m × 0.25 mm^2 Cyclodex-B column.

Preparation of proteins

Mutations of the desired residues were performed by the polymerase chain reaction-based technique. Heme proteins were expressed and purified according to previous reports.[33,49,62] The extraction of heme and incorporation of manganese(III) protoporphyrin IX to apomyoglobin were performed according to the literature.[26,35,63–65] All the mutants were confirmed by ESI-MS.

Kinetic studies with $KHSO_5$

The reactions were initiated by using 10 equiv. Oxone® (20 equiv. $KHSO_5$) in 50 mM potassium phosphate buffer, monitored by using a UV-vis spectrometer. The final concentration of protein was 30 μM reacting at 5 °C. The kinetic traces at 410 nm for Mn=O Por were used for calculating the pseudo first-order rates k_{obs} by fitting to a single-exponential eqn (1):

$$y = y_0 + a\ (1 - e^{-x/t}) \quad (1)$$

where x is the reaction time, and y is the absorbance at λ = 410 nm. $k_{obs} = -1/t$.

Docking of HSO_5^- and His3 Mb

Preparation of ligand and receptor. The His3 Mb protein scaffold was obtained from the Protein Data Bank (PDB code: 4FWZ). Before docking, water molecules were removed, and the HSO_5^- ion was optimized by using the Gaussian 09 package.[66] The optimization was performed by the DFT/B3LYP method, with the 6-31G (d) basis set for all atoms.

Docking. We performed docking of HSO_5^- into His3 Mb using AutoDock (version 4.2.3) and AutoDockTools (version 1.5.4). The grids (8.25 Å × 12.75 Å × 12 Å) were set around the heme-binding site containing the distal ligands and axial ligand. Three distal residues, His-29, His-43, and His-64, were set as flexible parts, other residues were considered to be rigid. In the docking program, the Lamarckian genetic algorithm method was used. The number of individuals in population was 150, the maximum number of energy evaluations was set as 2 500 000, and the maximum of generations was 27 000, and other parameters were used with default values.

EPR experiments

The EPR spectra were recorded at −170 °C in PBS buffer (pH 7.4). 1.0 mM protein was mixed with 20 equiv. H_2O_2 or 10 equiv. Oxone® (containing 20 equiv. $KHSO_5$) in buffer. The mixed solution was kept for 3 min and then frozen with liquid nitrogen for EPR measurement.

Styrene epoxidation

In the time course experiment, 0.2 mM proteins were mixed with 20 equiv. styrene in 50 mM potassium phosphate buffer (pH 7.4). The reactions were initiated with 10 equiv. Oxone®, reacting at 4 °C for 0–2 h. The reaction was quenched with 20 eq. $Na_2S_2O_3$ at a specific time. Then CH_2Cl_2 was added to extract the organic components. The CH_2Cl_2 solution was dried with anhydrous Na_2SO_4, concentrated to about 300 μL, and detected by GC. 20 equiv. of chlorobenzene were used as an internal reference. The epoxide product was also confirmed by ^1H NMR, and its retention time was confirmed by using styrene oxide purchased.

In the screening of different proteins, we use the same conditions and processes but quench the reaction after 1 h. The mixture was also extracted with CH_2Cl_2, dried with anhydrous Na_2SO_4, and detected by GC.

Acknowledgements

This project was supported by the National Scientific Foundation of China (grant no. 20971007, 21101169, 21271013, and 21571007) and the National Key Basic Research Support Foundation of China (NKBRSFC) (2010CB912302, 2015CB856300, and 2015CB856301).

Notes and references

1 J. Barber and J. W. Murray, *Coord. Chem. Rev.*, 2008, **252**, 233.
2 H. Dau and M. Haumann, *Coord. Chem. Rev.*, 2008, **252**, 273.
3 V. Daier, D. Moreno, C. Duhayon, J.-P. Tuchagues and S. Signorella, *Eur. J. Inorg. Chem.*, 2010, 965.
4 S. Signorella and C. Hureau, *Coord. Chem. Rev.*, 2012, **256**, 1229.
5 F. Campaci and S. Campestrini, *J. Mol. Catal. A: Chem.*, 1999, **140**, 121.
6 W. Nam, I. Kim, M. H. Lim, H. J. Choi, J. S. Lee and H. G. Jang, *Chem. – Eur. J.*, 2002, **8**, 2067.
7 H. M. Neu, T. Yang, R. A. Baglia, T. H. Yosca, M. T. Green, M. G. Quesne, S. P. De Visser and D. P. Goldberg, *J. Am. Chem. Soc.*, 2014, **136**, 13845.
8 P. Leeladee and D. P. Goldberg, *Inorg. Chem.*, 2010, **49**, 3083.
9 H. Srour, P. L. Maux and G. Simonneaux, *Inorg. Chem.*, 2012, **51**, 5850.
10 K. A. Prokop, H. M. Neu, S. P. De Visser and D. P. Goldberg, *J. Am. Chem. Soc.*, 2011, **133**, 15874.
11 R. J. Nick, G. B. Ray, K. M. Fish, T. G. Spiro and J. T. Groves, *J. Am. Chem. Soc.*, 1991, **113**, 1838.
12 K. K. Khan, M. S. Mondal and S. Mitra, *J. Chem. Soc., Dalton Trans.*, 1996, 1059.
13 K. K. Khan, M. S. Mondal and S. Mitra, *J. Chem. Soc., Dalton Trans.*, 1998, **4**, 533.

14 X. Wang and Y. Lu, *Biochemistry*, 1999, **38**, 9146.
15 A. Gengenbach, S. Syn, X. Wang and Y. Lu, *Biochemistry*, 1999, **38**, 11425.
16 D. W. Low, S. Abedin, G. Yang, J. R. Winkler and H. B. Gray, *Inorg. Chem.*, 1998, **37**, 1841.
17 C. Veeger, *J. Inorg. Biochem.*, 2002, **91**, 35.
18 J.-L. Primus, M. G. Boersma, D. Mandon, S. Boeren, C. Veeger, R. Weiss and I. M. C. M. Rietjens, *J. Biol. Inorg. Chem.*, 1999, **4**, 274.
19 J.-L. Primus, S. Grunenwald, P.-L. Hagedoorn, A.-M. Albrecht-Gary, D. Mandon and C. Veeger, *J. Am. Chem. Soc.*, 2002, **124**, 1214.
20 Z. N. Zahran, L. Chooback, D. M. Copeland, A. H. West and G. B. Richter-Addo, *J. Inorg. Biochem.*, 2008, **102**, 216.
21 I. Taniguchi, C.-Z. Li, M. Ishida and Q. Yao, *J. Electroanal. Chem.*, 1999, **460**, 245.
22 Y.-W. Lin, N. Yeung, Y.-G. Gao, K. D. Miner, S. Tian, H. Robinson and Y. Lu, *Proc. Natl. Acad. Sci. U. S. A.*, 2010, **107**, 8581.
23 N.-T. Yu and M. Tsubaki, *Biochemistry*, 1980, **19**, 4647.
24 F. Masuya and H. Hori, *Biochim. Biophys. Acta, Protein Struct. Mol. Enzymol.*, 1993, **1203**, 99.
25 J. L. Heinecke, J. Yi, J. C. M. Pereira, G. B. Richter-Addo and P. C. Ford, *J. Inorg. Biochem.*, 2012, **107**, 47.
26 M. S. Mondal, S. Mazumdar and S. Mitra, *Inorg. Chem.*, 1993, **32**, 5362.
27 M. S. Mondal and S. Mitra, *Biochim. Biophys. Acta*, 1996, **1296**, 174.
28 R. Lin, C. E. Immoos and P. J. Farmer, *J. Biol. Inorg. Chem.*, 2000, **5**, 738.
29 M. Horitani, H. Yashiro, M. Hagiwara and H. Hori, *J. Inorg. Biochem.*, 2008, **102**, 781.
30 K. L. Stone, J. Hua and H. Choudhry, *Inorganics*, 2015, **3**, 219.
31 M. Ohashi, T. Koshiyama, T. Ueno, M. Yanase, H. Fujii and Y. Watanabe, *Angew. Chem., Int. Ed.*, 2003, **42**, 1005.
32 K. Oohora, Y. Kihira, E. Mizohata, T. Inoue and T. Hayashi, *J. Am. Chem. Soc.*, 2013, **135**, 17282.
33 J.-L. Zhang, D. K. Garner, L. Liang, D. A. Barrios and Y. Lu, *Chem. – Eur. J.*, 2009, **15**, 7481.
34 D. K. Garner, L. Liang, D. A. Barrios, J.-L. Zhang and Y. Lu, *ACS Catal.*, 2011, **1**, 1083.
35 J. R. Carey, S. K. Ma, T. D. Pfister, D. K. Garner, H. K. Kim, J. A. Abramite, Z. Wang, Z. Guo and Y. Lu, *J. Am. Chem. Soc.*, 2004, **126**, 10812.
36 A. Tsai, C. Wei, H. K. Baek, R. J. Kulmacz and H. E. Van Wart, *J. Biol. Chem.*, 1997, **272**, 8885.
37 E. S. Ryabova and E. Nordlander, *Dalton Trans.*, 2005, 1228.
38 Y.-B. Cai, X.-H. Li, J. Jing and J.-L. Zhang, *Metallomics*, 2013, **5**, 828.
39 M. H. Gelb, W. A. Toscano Jr. and S. G. Sligar, *Proc. Natl. Acad. Sci. U. S. A.*, 1982, **79**, 5758.
40 S. Ozaki, T. Matsui and Y. Watanabe, *J. Am. Chem. Soc.*, 1996, **118**, 9784.
41 T. Matsui, S. Ozaki, E. Liong, G. N. Phillips Jr. and Y. Watanabe, *J. Biol. Chem.*, 1999, **274**, 2838.
42 T. Matsui, S. Ozaki and Y. Watanabe, *J. Am. Chem. Soc.*, 1999, **121**, 9952.
43 S. Ozaki, M. P. Roach, T. Matsui and Y. Watanabe, *Acc. Chem. Res.*, 2001, **34**, 818.
44 B. Meunier, *Chem. Rev.*, 1992, **92**, 1411.
45 D. Chatterjee, A. Sikdar, V. R. Patnam, A. Theodoridis and R. van Eldik, *Dalton Trans.*, 2008, 3851.
46 J. T. Groves, J. Lee and S. S. Marla, *J. Am. Chem. Soc.*, 1997, **119**, 6269.
47 N. Jin and J. T. Groves, *J. Am. Chem. Soc.*, 1999, **121**, 2923.
48 K. D. Miner, A. Mukherjee, Y.-G. Gao, E. L. Null, I. D. Petrik, X. Zhao, N. Yeung, H. Robinson and Y. Lu, *Angew. Chem., Int. Ed.*, 2012, **51**, 5589.
49 J. L. Anderson, J. Ding, R. D. McCulla, W. S. Jenks and D. W. Armstrong, *J. Chromatogr. A*, 2002, **946**, 197.
50 H. M. Neu, R. A. Baglia and D. P. Goldberg, *Acc. Chem. Res.*, 2015, **48**, 2754.
51 P. Leeladee, R. A. Baglia, K. A. Prokop, R. Latifi, S. P. De Visser and D. P. Goldberg, *J. Am. Chem. Soc.*, 2012, **134**, 10397.
52 C. J. Bougher, S. Liu, S. D. Hicks and M. M. Abu-Omar, *J. Am. Chem. Soc.*, 2015, **137**, 14481.
53 N. Jin, J. L. Bourassa, S. C. Tizio and J. T. Groves, *Angew. Chem., Int. Ed.*, 2000, **39**, 3849.
54 T. Yonetani and T. Asakura, *J. Biol. Chem.*, 1969, **244**, 4580.
55 H. Hori, M. Ikeda-Saito and T. Yonetani, *Biochim. Biophys. Acta*, 1987, **912**, 74.
56 A. J. Allentoff, J. L. Bolton, A. Wilks, J. A. Thompson and P. R. Ortiz de Montellano, *J. Am. Chem. Soc.*, 1992, **114**, 9744.
57 D. E. Lansky and D. P. Goldberg, *Inorg. Chem.*, 2006, **45**, 5119.
58 D. Janardanan, D. Usharani and S. Shaik, *Angew. Chem., Int. Ed.*, 2012, **51**, 4421.
59 C. Crestini, A. Pastorini and P. Tagliatesta, *Eur. J. Inorg. Chem.*, 2004, 4477.
60 A. Rezaeifard, M. Jafarpour, S. Rayati and R. Shariati, *Dyes Pigm.*, 2009, **80**, 80.
61 Y.-W. Lin, S.-S. Dong, J.-H. Liu, C.-M. Nie and G.-B. Wen, *J. Mol. Catal. B: Enzym.*, 2013, **91**, 25.
62 J. A. Sigman, B. C. Kwok and Y. Lu, *J. Am. Chem. Soc.*, 2000, **122**, 8192.
63 B. A. Springer and S. G. Sligar, *Proc. Natl. Acad. Sci. U. S. A.*, 1987, **84**, 8961.
64 F. W. J. Teale, *Biochim. Biophys. Acta*, 1959, **35**, 543.
65 W. R. Fisher, H. Taniuchi and C. B. Anfinsen, *J. Biol. Chem.*, 1973, **248**, 3188.
66 M. J. Frisch, G. W. Trucks, H. B. Schlegel, G. E. Scuseria, M. A. Robb, J. R. Cheeseman, G. Scalmani, V. Barone, B. Mennucci, G. A. Petersson, H. Nakatsuji, M. Caricato, X. Li, H. P. Hratchian, A. F. Izmaylov, G. Z. J. Bloino, J. L. Sonnenberg, M. Hada, M. Ehara, K. Toyota, R. Fukuda, J. Hasegawa, M. Ishida, T. Nakajima, Y. Honda, O. Kitao, H. Nakai, T. Vreven, J. J. A. Montgomery, J. E. Peralta, F. Ogliaro, M. Bearpark, J. J. Heyd, E. Brothers, K. N. Kudin, V. N. Staroverov, R. Kobayashi, J. Normand,

K. Raghavachari, A. Rendell, J. C. Burant, S. S. Iyengar, J. Tomasi, M. Cossi, N. Rega, J. M. Millam, M. Klene, J. E. Knox, J. B. Cross, V. Bakken, C. Adamo, J. Jaramillo, R. Gomperts, R. E. Stratmann, O. Yazyev, A. J. Austin, R. Cammi, C. Pomelli, J. Ochterski, R. L. Martin, K. Morokuma, V. G. Zakrzewski, G. A. Voth, P. Salvador, J. J. Dannenberg, S. Dapprich, A. D. Daniels, O. Farkas, J. B. Foresman, J. V. Ortiz, J. Cioslowski and D. J. Fox, *GAUSSIAN 09 (Revision A.2)*, Gaussian, Inc., Wallingford, CT, 2009.

